Quantum Electronics **48** (6) 516–520 (2018)

INTERACTION OF LASER RADIATION WITH MATTER https://doi.org/10.1070/QEL16650

Acoustic signal investigation in the ice melting under high-power laser irradiation at a wavelength of 2940 nm

N.N. Il'ichev, A.V. Sidorin, E.S. Gulyamova, P.P. Pashinin

Abstract. **We have measured acoustic signals emerging in the melting of a thin (about 2 μm) ice layer, which is sandwiched between two substrates, under high-power laser irradiation at a wavelength of 2940 nm. A negative-pressure acoustic signal arising from the difference in the specific volumes of water and ice was found to occur in the ice melting. The amplitude of this signal was comparable to the amplitude of the positive-pressure signal produced under laser irradiation of the same layer of water. The shapes of acoustic signals were measured for different energy densities of the incident radiation. The variation of negative-pressure pulse shape with increasing radiation energy density was interpreted as a continuity break of the medium. The temperature and pressure in the layer were estimated in the heating of water and the melting of ice.**

Keywords: *optoacoustics, laser-induced ice melting, acoustic sensors.*

1. Introduction

Acoustic methods of investigation into the melting of solids under high-power laser irradiation make it possible to observe phase transformations with temporal resolution. This is of interest for the investigation of dynamics of the processes occurring during melting, in particular the liquid–solid phase ratio in the course of melting, as well as for the observation of metastable states. This is particularly important in the case of bulk heating, which takes place, for instance, in the laser heating of substances that are relatively transparent to the heating radiation, when the heat is released throughout their volume rather than transferred to the interphase boundary by thermal conduction.

There are papers concerned with the investigation of substance melting under laser irradiation with the use of acoustic methods. For instance, Karabutov et al. [1] outlined the results of investigations into the optoacoustic effect in the melting of indium residing under a substrate transparent to the heating radiation. Since the solid indium density exceeds the liquid one, the melting is accompanied by a pressure increase. However, the pressure also rises in the heating of indium (due to its thermal expansion), and therefore the melting has only a qualitative effect on the temporal dependence of the pressure, which is a matter of some difficulty in the experimental determination of the instant of onset of the phase transition. It is noteworthy that laser radiation with a wavelength close to 1000 nm is absorbed in a very thin (~50 nm [1]) indium layer. For a laser pulse duration of ~10 ns, the heat diffusion depth in indium amounts to about 700 nm. Comparing this figure to the radiation absorption depth suggests that we are not dealing with bulk substance heating in the case of laser heating of the metal.

Several published works were dedicated to the investigation of sound generation in the phase transitions occurring under laser irradiation. For instance, Mazhukin et al. [2] investigated theoretically the dynamics of fast processes in the melting and evaporation of a substance in the zone of laser heating. The case of exposing a metal to laser irradiation was also considered in that paper. The results of investigation of the dynamic shift of the metal boiling point under laser irradiation were outlined in Ref. [3]. The photoacoustic effects occurring in the laser irradiation of a substance were investigated in Refs [4, 5]. In all papers listed above the phase transition occurred either in the metal melting or in the vaporisation of the substance by high-power laser radiation.

One of the purposes of our work is to record and investigate the acoustic signals produced in the melting of a thin ice layer, which is sandwiched between two substrates, by high-power laser radiation with a wavelength of 2940 nm.

Also considered was the feasibility of using acoustic signals generated in the melting of ice for the calibration of pulsed acoustic sensors.

2. Experiment

The experiment is schematically represented in Fig. 1. Use was made of two types of substrates to cover the layer of water or ice: 5.7-mm thick fused silica substrates and 9.5-mm thick sapphire substrates.

These materials are chosen due to a large difference of their thermal conductivities and acoustic impedances, so that it is of interest to compare the characteristics of acoustic signals from a layer of water or ice with the use of these substrates.

The cooling was affected by blowing the vapour of liquid nitrogen, which was produced by its evaporation from a Dewar vessel, on substrate (*4*) and the upper part of acoustic sensor (AS) (*6*). The AS and the substrate were so arranged that laser radiation propagated vertically, the upper part of the glass of foamed plastics was not closed, and the 'dry' (free of water vapour) cool nitrogen flew freely from the glass, not letting the water vapour of the ambient air freeze on the substrate. The laser radiation passed through this domain with-

N.N. Il'ichev, A.V. Sidorin, E.S. Gulyamova, P.P. Pashinin
A.M. Prokhorov General Physics Institute, Russian Academy of Sciences, ul. Vavilova 38, 119991 Moscow, Russia;
e-mail: ilichev@kapella.gpi.ru

Received 21 February 2018
Kvantovaya Elektronika **48** (6) 516–520 (2018)
Translated by E.N. Ragozin

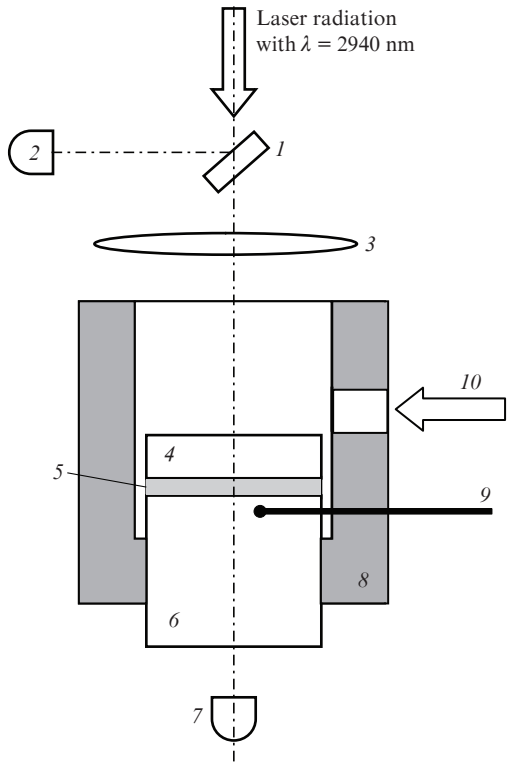

Figure 1. Schematic of the setup:
(*1*) beam splitter substrate; (*2*, *7*) PD29 photodetectors; (*3*) BaF_2 lens with f = 300 mm; (*4*) substrate; (*5*) water or ice layer of thickness ~2 μm; (*6*) acoustic sensor of lithium niobate; (*8*) glass of foamed plastics; (*9*) temperature sensor; (*10*) flow of liquid nitrogen vapour.

out attenuation. The temperature was monitored with a temperature-sensitive element, which was in thermal contact with the crystal of lithium niobate near the water layer.

An Er:YAG crystal laser was actively Q-switched, the highest energy density on the layer surfaces amounted to 0.26 J cm^{-2}, the radiation spot area was equal to 0.037 cm^2, and the pulse duration was equal to ~275 ns. The transverse radiation intensity distribution was close to the Gaussian one. For the ~2940-nm radiation the absorption coefficient in water and ice is equal to ~1.3×10^4 cm^{-1} [6], and therefore the heating of a 1–2 μm thick layer by this radiation may be thought of as being bulk heating.

The acoustic sensor was a lithium niobate crystal parallelepiped with 25-, 25-, and 35-mm long edges parallel to the crystallographic axes Y, X, and Z, respectively. The side surface of the sensor was thermally insulated with mounting foam. A round signal electrode of ~1-μm thick copper foil with a pickup area ~3 mm in diameter resided on the upper surface of the crystal and contacted directly with water or ice. The second grounded electrode resided on the opposite side of the crystal. The selected crystal dimensions and electrode arrangement permitted shifting in time the onset of parasitic signals caused by reflections of the acoustic wave propagating inside the crystal. The signal was recorded with a DPO 7254 oscilloscope. The acoustic sensor was capable of recording pressure variations with a 7-ns period of the intermode beats of laser intensity. Since the thin layer of water or ice was in direct contact with the signal electrode, we were not concerned about the diffraction distortion of the shape of acoustic wave in its propagation through the medium. The existence of such a distortion was pointed out in Refs [4, 7]. The water layer thickness was estimated at ~2 μm from the transmittance to the λ = 2940 nm radiation. Distilled water was used in our experiments.

3. Experimental results

Figure 2 shows the time dependences of the acoustic signals with the use of fused silica and sapphire substrates to cover the layers of water and ice. The radiation energy density was equal to 0.26 J cm^{-2}, the water temperature was close to 20 °C, the ice temperature prior to the arrival of a laser pulse ranged from –5 to –10 °C. The oscilloscope sweep duration was selected so as to make visible the peaks emerging due to the reflection of acoustic signals from the free substrate surface. The signals arising from the acoustic pulse propagation and reflection in the sensor are not seen on this time scale.

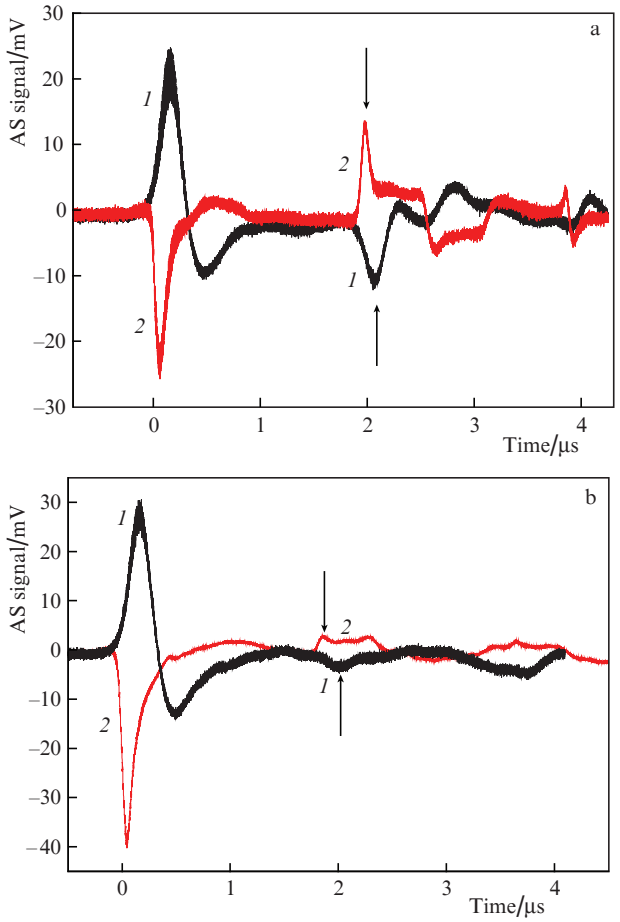

Figure 2. AS signals with the use of (a) fused silica and (b) sapphire substrates covering the layers of (*1*) water and (*2*) ice. The arrows indicate the peaks emerging due to the reflection of acoustic signals from the free substrate surface. The energy density of laser radiation: 0.26 J cm^{-2}.

The polarity of acoustic signal from the water layer is positive and that from the ice layer is negative, i.e. the pressure produced in the water layer under irradiation is positive and that in the ice layer under irradiation is negative. In the latter case the negative signal is indicative of ice melting, and the negative pressure pulse is generated, since the water density is higher than the ice density.

Interestingly, the trailing edge of negative pressure pulses decreases rather steeply [Figs 2a and 2b, curves (*2*)], which

may be indicative of the break of continuity of ice or water, since a mixture of water and ice is produced in the melting. The possibility that the continuity break does occur is confirmed by the fact that the shape of acoustic pressure pulse reflected in the substrate in the case of ice layer is much different the shape of the pressure pulse in this layer (see, for instance, Fig. 2a). Both for water and for ice, the diffraction shape distortion of the signal in its propagation in the substrate may be an additional factor that distorts the reflected pulse shape.

Figure 3 shows the time dependences of the pressure pulse for different radiation energy densities in the cases when the ice layers were covered by substrates of fused silica and sapphire. One can see that the amplitude of the pressure pulse decreases in magnitude with decreasing radiation energy density. With reference to Fig. 3, the pressure is positive at the onset of the radiation pulse, which is attributable to the generation of a photoacoustic signal due to ice heating. Next, with the onset ice melting, a negative pressure pulse is generated. It is noteworthy that the amplitude of the signal from the ice layer under the sapphire substrate is 1.5–2 times higher than in the case of fused silica substrate.

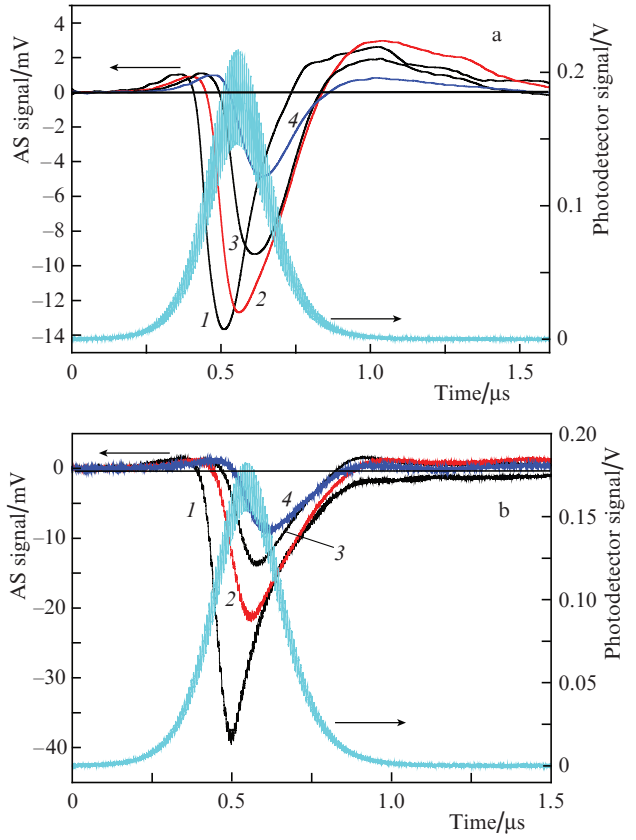

Figure 3. AS signals in the irradiation of an ice layer covered by (a) fused silica and (b) sapphire substrates. Radiation energy density: (*1*) 0.26, (*2*) 0.13, (*3*) 0.08 and (*4*) 0.05 J cm^{-2}. The high-frequency component of the acoustic signal is filtered out in Fig. 3a. Also shown are signals from photodetector (*2*) (see Fig. 1).

4. Discussion of results

Let us estimate the temperature, the pressure, and the thickness variation of a water layer irradiated by $\lambda = 2940$ nm radiation. For a rough estimate we assume that the temperature and the pressure inside the water layer are independent of the coordinate perpendicular to the layer plane. Let a pulse of laser radiation with a duration τ_p and an energy density E on the layer surface be incident on the water layer of thickness h, which resides between a lithium niobate crystal (medium 1) and a fused silica substrate (medium 2). The radiation intensity distribution over the cross section of the laser beam is assumed to be rectangular. The energy absorbed in the water layer is spent to heat it, to heat media 1 and 2, which confine the layer, and the copper electrode of thickness $h_{Cu} = 1$ μm. We also assume that the surface temperature of media 1 and 2 is equal to the layer temperature and that their heat penetration depth is equal to the thermal diffusion depth. Since the heat propagates in the electrode in a time of ~9 ns, the electrode temperature is assumed to be equal to the water temperature for $\tau_p = 275$ ns. Under these conditions, the energy balance is written as follows:

$$E[1-\exp(-\alpha h)] = C_w\rho_w h\Delta T + \sqrt{C_1\rho_1\chi_1\tau_p}\,\Delta T$$

$$+\sqrt{C_2\rho_2\chi_2\tau_p}\,\Delta T + C_{Cu}\rho_{Cu}h_{Cu}\Delta T,$$

where C, χ, and ρ are the specific heats, thermal conductivities, and densities of the water (subscript w), the crystal and the substrate (subscripts 1 and 2) confining the water layer, and the electrode (subscript Cu); and ΔT is the layer temperature variation. As a result,

$$\Delta T = \frac{E[1-\exp(-\alpha h)]}{C_w\rho_w h + \sqrt{C_1\rho_1\chi_1\tau_p} + \sqrt{C_2\rho_2\chi_2\tau_p} + C_{Cu}\rho_{Cu}h_{Cu}}. \quad (1)$$

Assuming that the radiation is completely absorbed in the layer, from formula (1) we conclude that the water layer temperature variation for $E = 0.26$ J cm^{-2} and $\tau_p = 275$ ns amounts to 175 °C (fused silica substrate) and 143 °C (sapphire substrate). The temperature difference in these cases is attributable to the higher thermal conductivity of sapphire.

The characteristics of the materials in use are collected in Table 1. The data were borrowed from Ref. [8]. The acoustic wave travel time through the 1-μm thick electrode is equal to ~0.2 ns, and the pressures inside the copper electrode and the water are therefore assumed to be equal. Under the action of pressure Δp the elastic wall 1, which limits the layer, moves at a velocity $\Delta p/(V_{s1}\rho_1)$ [9], where V_{s1} is the sound velocity in medium 1. The variation rate of layer thickness h

$$\frac{dh}{dt} = \Delta p\left(\frac{1}{z_1} + \frac{1}{z_2}\right),$$

Table 1.

Material	Specific heat/ kJ kg^{-1} °C^{-1}	Density/ 10^3 kg m^{-3}	Thermal conductivity/ W m^{-1} °C^{-1}	Sound velocity/ m s^{-1}
Water	4.2	1	0.5	1400
Ice	2.12	0.917	2.21	3800
$LiNbO_3$	0.657	4.7	4.6	7200
Fused silica	1.05	2.2	1.38	5900
Sapphire	0.756	3.97	23.1	11000
Copper	0.39	8.93	400	4700

where $z_1 = V_{s1}\rho_1$; and $z_2 = V_{s2}\rho_2$. The variation of layer thickness due to the deformation of the layer-confining media during the course of the laser pulse is as follows:

$$\Delta h = \Delta p\left(\frac{1}{z_1} + \frac{1}{z_2}\right)\tau_p. \quad (2)$$

The volume variation of the water layer

$$dV = \left(\frac{\partial V}{\partial p}\right)_T dp + \left(\frac{\partial V}{\partial T}\right)_p dT.$$

Hence we obtain the equation for the variation of the layer thickness:

$$\Delta h = h(\beta_w \Delta p + \gamma_w \Delta T), \quad (3)$$

where

$$\beta_w = \frac{1}{V}\frac{\partial V}{\partial p} \text{ и } \gamma_w = \frac{1}{V}\frac{\partial V}{\partial T}$$

are the compressibility and the volume thermal expansion coefficient of water, respectively. The sound travel time in the transverse direction exceeds 700 ns (the radius of irradiated spot on the layer: ~1 mm), which is nearly two times longer than the duration of the laser pulse. We therefore assume that only the layer thickness varies, $dV = Sdh$. Considering that $\tau_p(z_1^{-1} + z_2^{-1}) \gg h|\beta_w|$, from formulas (2) and (3) we obtain the pressure variation

$$\Delta p = \frac{h\gamma_w \Delta T}{\tau_p(z_1^{-1} + z_2^{-1})}. \quad (4)$$

The value of Δh is found from formula (2). Calculation by formulas (2)–(4) for h = 2 μm yields a pressure of 14 MPa (138 atm) and Δh = 0.4 μm when the layer is confined by the fused silica substrate and Δh = 0.26 μm in the case of the sapphire substrate. The volume expansion coefficient of water depends on the temperature and the pressure. In the calculation we assumed that $\gamma_w = 1.13\times10^{-3}$ °C^{-1} at a temperature of 175 °C and a pressure of 14 MPa (fused silica substrate) and that $\gamma_w = 0.93\times10^{-3}$ °C^{-1} at a temperature of 143 °C and a pressure of 18 MPa (sapphire substrate). The volume expansion coefficients of water were found using the formulas given in Ref. [10]. The work of the pressure force to move the walls was neglected in the determination of temperature variation by formula (1). This is admissible in the present case, because, according to calculations, this work is small in comparison with the energy spent to heat the water.

Let us estimate the pressure variation in the melting of ice under irradiation. The layer thickness variation in the ice melting is caused by the medium's density variation in the melting and by the volume variation under the variation of the pressure. The volume variation due to the temperature variation may be neglected: we assume that the melting takes place at a constant temperature. As follows from the Clausius–Clapeyron equation, the melting temperature of ice changes by –1 °C with increasing pressure by 134 atm [11]. We assume that the transverse dimensions of the layer remain invariable to obtain

$$\Delta h = h\beta\Delta p + h\left(\frac{\rho_i}{\rho_w} - 1\right), \quad (5)$$

where subscript i refers to ice and β is the average compressibility of the ice–water mixture. On the other hand, the layer thickness variation due to the deformation of the layer-confining media is described by expression (2). considering that in our conditions the inequality $\tau_p(z_1^{-1} + z_2^{-1}) \gg h|\beta|$ is fulfilled both for the compressibilities of ice and water, from formulas (2) and (5) we obtain

$$\Delta p = \frac{h(\rho_i/\rho_w - 1)}{\tau_p(z_1^{-1} + z_2^{-1})}. \quad (6)$$

When the layer is confined by the fused silica substrate, calculation with the use of formula (6) gives Δp = –5.7 MPa (–56 atm), and from expression (2) we obtain Δh = – 0.17 μm. Similarly, in the case of sapphire substrate Δp = –11.5 MPa (–114 atm) and Δh = –0.16 μm. A comparison of the calculated values of the negative pressure in the melting of ice under the fused silica and sapphire substrates shows that the pressure is nearly two times higher in the sapphire substrate case. From the experimental data for the minimal pressure in the melting of ice shown in Figs 2a and 2b it also follows that the pressure under the sapphire substrate is 1.5–2 times higher in magnitude than under the fused silica substrate.

We also note that melting a 2-μm thick ice layer requires a radiation energy density of ~0.06 J cm^{-2} (neglecting the heat escape to the substrates and the electrode). When the energy density exceeds this value, the pressure should not decrease, since all ice should melt. However, as is clear from Fig. 3 the amplitude of the pressure signal continues to grow in magnitude. This is indication that the theoretical model in use is too coarse and calls for improvement.

During the course of the radiation pulse, the ice melts, and after its complete melting the resultant water would be heated by the energy contained in the remaining part of the laser pulse. The pressure in the layer should rise due to the water heating. According to calculations, for E = 0.2 J cm^{-2} the pressure in the water layer under the fused silica substrate should rise by 11 MPa (112 atm) and by 12 MPa (116 atm) under the sapphire substrate. When it is considered that the layer pressure is negative after the melting of ice, after the water heating the pressure should become positive and equal to 5.3 MPa (52 atm) (fused silica substrate) and to 0.5 MPa (5 atm) (sapphire substrate). This signifies that the negative pressure pulse in the melting of ice must end with a positive pressure jump. However, as is clear from Fig. 2, this pulse does not occur, which is another indirect indication of the layer continuity break.

Note that the radiation energy density does not appear in expression (6) and that all quantities in it are either determined experimentally or known from the reference literature. That is why the acoustic signal produced in the melting of ice may be used for the calibration of acoustic sensors. All that must to be provided is the complete melting of the ice.

5. Conclusions

We have measured the AS signals emerging in the exposure of a thin water or ice layer under a fused silica or sapphire substrate to high-power radiation with λ = 2940 nm. The negative acoustic signal produced in the irradiation of the ice layer by the high-power laser radiation is interpreted as negative pressure, which results from the ice melting due to the difference between the specific volumes of ice and water. The temporal shape of the AS signals in the irradiation of the ice layer at a

laser energy density of 0.26 J cm^{-2} allows a conclusion that a continuity break in the layer under irradiation might occur under the action of the negative pressure.

We estimated the temperature and the pressure in the water and ice layers irradiated by laser pulses with an energy density of 0.26 J cm^{-2}. Their average values for water: ΔT = 175 °C, Δp = 14 MPa (138 atm) (fused silica substrate) and ΔT = 143 °C, Δp = 18 MPa (181 atm) (sapphire substrate). For ice, Δp = –55 atm (fused silica substrate) and Δp = –112 atm (sapphire substrate). As our calculations suggest, the pressure under the sapphire substrate is higher (in magnitude for ice) than under the fused silica substrate owing to the higher acoustic impedance of sapphire.

We propose the use of acoustic signals generated in the melting of ice for the absolute calibration of pulsed acoustic sensors.

Acknowledgements. This work was partly supported by the Russian Foundation for Basic Research (Grant No. 16-02-00807a) and the Program I.7 of the Presidium of the Russian Academy of Sciences 'Topical photonics problems, probing nonuniform media and materials'.

References

1. Karabutov A.A., Kubyshkin A.P., Panchenko V.Ya., et al. *Quantum Electron*., **28** (8), 670 (1998) [*Kvantovaya Elektron.*, **25** (8), 690 (1998)].
2. Mazhukin V.I., Nikiforova N.M., Samokhin A.A. *Trudy IOFAN*, **60**, 108 (2004).
3. Karabutov A.A., Kubyshkin A.P., Panchenko V.Ya., Podymova N.B. *Quantum Electron.*, **25** (8), 789 (1995) [*Kvantovaya Elektron*., **22** (8), 820 (1995)].
4. Gusev V.E., Karabutov A.A. *Lazernaya optoakustika* (Laser Optoacoustics) (Moscow: Nauka, 1991).
5. Paltauf G., Dyer P.E. *Chem. Rev*., **103**, 487 (2003).
6. Zolotarev V.M., Morozov V.N., Smirnova E.V. *Opticheskie postoyannye prirodnykh i tekhnicheskikh sred. Spravochnik* (Optical Constants of Natural and Technical Media. Reference Book) (Leningrad: Chemistry, 1984).
7. Burmistrova L.V., Karabutov A.A., Portnyagin A.I. et al. *Akust. Zh*., **24** (5), 655 (1978).
8. Grigoriev I.S., Meilikhov E.Z. (Eds) *Handbook of Physical Quantities* (Boca Raton: CRC Press, 1997; Moscow: Energoatomizdat, 1991).
9. Krasil'nikov V.A., Krylov V.V. *Vvedenie v fizicheskuyu akustiku. Uchebnoe posobie* (Introduction to Physical Acoustics. Textbook) (Moscow: Nauka, 1984).
10. http://www.iapws.org/relguide/IF97-Rev.pdf.
11. Fermi E. *Thermodynamics* (New York: Prentice-Hall, 1937; Khar'kov: Izd. KhGU, 1969).